Int. J. Electrochem. Sci., 12 **(2017)** 5492 – 5502, doi: 10.20964/2017.06.55

International Journal of ELECTROCHEMICAL SCIENCE
www.electrochemsci.org

A Non-Enzymatic Glucose Sensor Based on Pd-Fe/Ti Nanocomposites

Chen Yang, Xiaolu Cui, Kaili Wang, Yu Cao[*]*, Chengyin Wang*[*] *and Xiaoya Hu*

College of Chemistry and Chemical Engineering, Jiangsu Key Laboratory of Environmental Engineering and Monitoring, Yangzhou University, 180 Si-Wang-Ting Road, Yangzhou, 225002, China.
[*]E-mail: yucao@yzu.edu.cn, wangcy@yzu.edu.cn

Received: 5 January 2017 / *Accepted:* 18 February 2017 / *Published:* 12 May 2017

A novel non-enzyme glucose sensor is constructed based on the three-dimensional Pd-Fe networks deposited on Ti substrates directly by a one-step chemical reduction method in aqueous solutions. Scanning electron microscopy (SEM) and energy-dispersive spectrometry (EDS) were used to characterize the as-synthesized nanoporous Pd-Fe composites. Amperometric and voltammetric methods were applied to evaluate the electrocatalytic activity of the modified electrodes toward non-enzymatic glucose oxidation in a 0.50 M NaOH at selected potentials. The prepared Pd-Fe/Ti electrode exhibits an excellent electrocatalytic activity, a wide linear range for glucose concentration from 2.0×10^{-3} to 3.0 mM (R = 0.9981), the sensitivity is 3.2×10^{2} μA mM^{-1} cm^{-2}, and the detection limit was found to be 1.0×10^{-3} mM (S/N = 3). It also shows good anti-interference capability in the presence of uric acid (UA), ascorbic acid (AA) and 4-acetamidophenol (AP). These results indicate that this Pd-Fe/Ti electrode has a potential application as a non-enzyme glucose sensor.

Keywords: nanoparticles, glucose, non-enzyme sensor, cyclic voltammetry, chronoamperometric.

1. INTRODUCTION

In recent years, glucose sensors have been extensively applied in health care, biological process, food industry and environmental monitoring [1]. To date, even though chromatographic [2] and spectroscopic [3] methods have been used for glucose testing, electrochemical method is the most dominating technology owing to selective recognition, accuracy, speed and low cost [4-5]. The first enzyme electrode was found in 1962 [6], researches of novel glucose sensors have been focusing on the pursuit of fast reaction, long operating life, high selectivity and high sensitivity. Compared with

enzyme sensors, non-enzymatic sensors can oxidize the glucose directly to avoid the drawbacks of enzymatic sensors including sufficient stability, good reproducibility, and simplicity of operation [7-8].

Nano-metallic materials, such as nanoporous Pd particles [9] and gold nanostructure [10], are recognized as promising raw and processed materials for fabricating electrochemical non-enzyme glucose sensors originating from their high active surface area, high biological compatibility and numbers of active sites [11]. Surprisingly, it had been demonstrated that multi-metallic catalysts such as Pt-Pd nanoflakes [12] and Au@Pd core-shell nanoparticles [13] can enhance the electrocatalytic activity for glucose sensing attribute to the beneficial synergistic effects [14]. Meanwhile, many nanostructured materials, with unique physical and chemical properties, have been used as the backbones of catalysts (for instance, nanowires (NWs) [15], carbon nanotubes (CNTs) [16], silicon nanowires (SiNWs) [17]). In addition, the graphene oxide (GO) [18] possess excellent electrocatalytic performance which should not be ignored. An increasing number of investigations have concentrated on the synthesis of various nanocomposites and their applications in non-enzymatic glucose analysis in recent years [19-22]. Interestingly, Wang [23] reported a Ti plate that can be regarded as the backbones of catalysts as well as a replacement of glassy carbon electrode based on its good conductivity, rough surface.

According to our survey, there were few reports about the synthesis of Pd-Fe materials on Ti plates in the preparation of non-enzymatic sensors till now. In this work, we investigate the electrochemical properties of non-enzymatic glucose sensor based on nanoporous Pd/Ti and Pd-Fe/Ti electrodes with active surfaces. The result shows that these electrodes can detect glucose with good sensitivity and selectivity.

2. EXPERIMENTAL SECTION

2.1 Materials

Pd chloride ($PdCl_2$), ferric trichloride ($FeCl_3$), glucose, sodium hydroxide (NaOH), sodium borohydride ($NaBH_4$) ascorbic acid (AA), uric acid (UA) and 4-acetamidophenol (AP) were purchased from Sinopharm Group Chemical Reagent Co. Ltd (http://www.instrument.com.cn/). Serum was obtained from the hospital of Yangzhou University (Yangzhou, China). Ti plates (15mm × 10 mm × 0.5 mm, 99.2 %) were purchased from Alfa Aesar (http://www.labgogo.com/). All other chemicals were of analytical grade, and all aqueous solutions were prepared in doubly distilled water.

2.2 Instruments

The surface morphology and composition of the synthesized samples were characterized using scanning electron microscopy (SEM) (S-4800, HITACHI) equipped with an energy-dispersive spectrometer (EDS). All electrochemical experiments were finished by electrochemical workstation (CHI800A, CH instrument Inc.). A conventional three-electrode system consisting of a saturated calomel electrode (SCE) as a reference, large platinum foil as a counter electrode, the Pd standard

electrode and the prepared nanoporous Pd/Ti or Pd-Fe/Ti as working electrode respectively. Unless otherwise specified, all potentials reported in this paper are referred to SCE.

2.3 Synthesis of Nanoporous Pd/Ti and Pd-Fe/Ti electrodes

The Pd-Fe/Ti electrode was prepared by a simple, one-pot and facile chemical reduction method. In a typical synthesis, Ti plates were immersed into the aqueous solutions of Pd and Pd-Fe particles, and sodium borohydride was used as reducing agent under optimal temperature and reagent concentration. Prior to the experiment, a series of operations were carried out not only to clear the oxide layer and organic matter on the Ti plates, but also to roughen the Ti surface. Firstly, Ti plates (15 mm × 10 mm × 0.5 mm) were sonicated in mixing solution of alcohol and acetone (1:1 in volume) for 20 min, followed in pure water for 20 min. Then, the Ti plates were etched in the solution of HCl (18 wt %) at 85 °C for 20 min and sonicated in pure water for 20 min. The etched Ti plate was placed in a beaker containing 1 ml (5 mM) H_2PdCl_4 solution and 3 ml H_2O in ice bath. In the case of Pd-Fe networks, the mixture solution also contained $PdCl_2$ and $FeCl_3$ (95:5 in volume) at concentrations that were stoichiometric to Pd, then add 1 ml 75 mM $NaBH_4$ solution with stirring. The coated Ti plates were removed after 8 h, dried in constant temperature drying oven at 85 °C for 2 h, and then rinsed with the pure water.

2.4 Electrochemical Experiments

Electrochemical experiment was carried out by the cyclic voltammograms (CVs) and amperometric technique. The potential range of CVs was from -0.8 to 0.2 V, and scan rate was 50 mV/s. Amperometric measurements of glucose were carried out in a 0.5 M NaOH at -20 mV. Currents at each addition of glucose every 50 s were recorded with the solution stirring constantly. The current densities were calculated by the surface area of electrodes. All measurements were operated at room temperature (22 ± 2 °C).

3. RESULTS AND AISCUSSION

3.1 Characterization of Pd-Fe/Ti electrodes

To investigate the surface morphology, the prepared electrodes Ti, Pd/Ti and Pd-Fe/Ti are examined by SEM. Fig. 1(a) and Fig. 1(b) show the SEM images of Ti plates before and after eatching. Fig. 1(c) indicates that the surface of Ti plate is totally covered by Pd nanoparticles, all the sample surfaces have irregular pores ranging from 10 to 20 nm in diameter, which are combined with each other to form a three-dimensional structure. The porous structure make the particles immobilize on the Ti surface stably. However, as can be seen in Fig. 1(e), the new feature is that the Pd-Fe catalysts possess flower shaped morphologies, except the smaller diameter. It has been reported that the

introduction of a trace amount of Fe^{3+} species could result in the formation of single crystal Pd from nanoparticles to nanobelts [24].

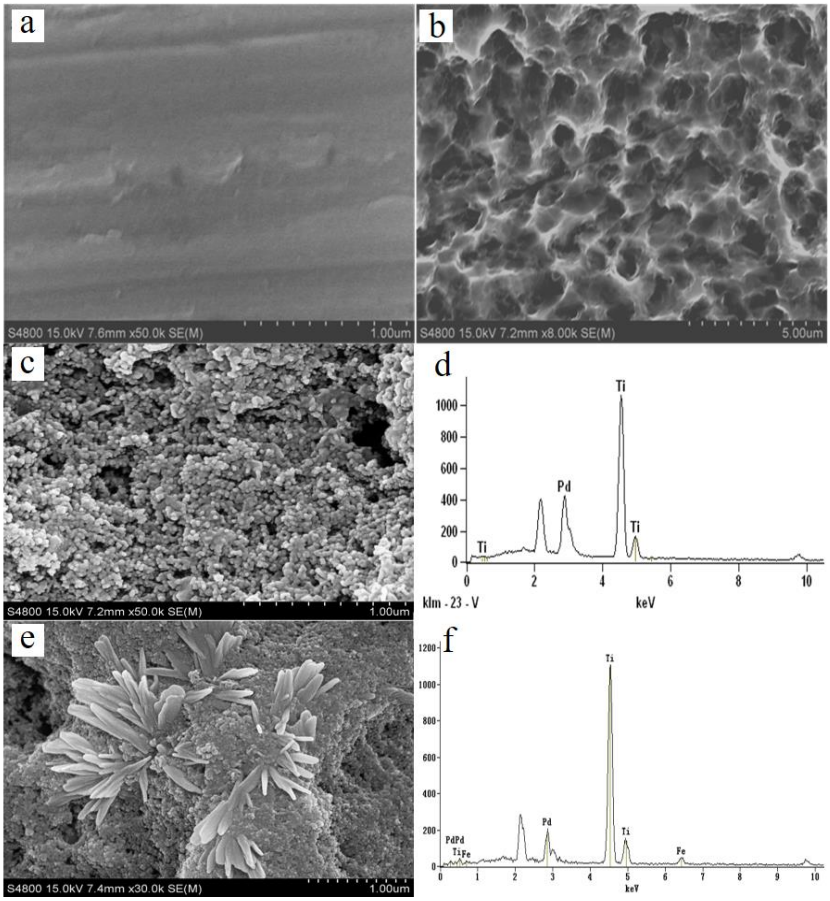

Figure 1. SEM images of Ti (a, b), Pd/Ti (c) and Pd-Fe/Ti (e), EDS of Pd/Ti (d) and Pd-Fe/Ti (f).

The elemental compositions of the prepared Pd/Ti and Pd-Fe/Ti were examined by EDS study, attached with SEM. Obviously, Fig. 1(d) displays the EDS spectrum of Pd/Ti material, we can find that there are several peaks only related to Pd and Ti, and without any other element in the observed spectrum. Meanwhile, Fig. 1(f) shows that the prepared Pd-Fe/Ti only has the peaks of Pd, Fe and Ti. The high intensity of EDS describes that the prepared Pd/Ti and Pd-Fe/Ti are pure without significant impurity.

3.2 Electro-oxidation behavior of glucose at Pd-Fe/Ti electrodes

Here, the electrocatalytic activity of a Pd standard electrode, Pd/Ti and Pd-Fe/Ti were investigated and compared by cyclic voltammetry at a scan rate 50 mV/s in 0.5 M NaOH without glucose (Fig. 2(a)) and with glucose (Fig. 2(b)). Ti plate was chosen as the substrate due to its good electrical conductivity, low cost and high catalytic activity.

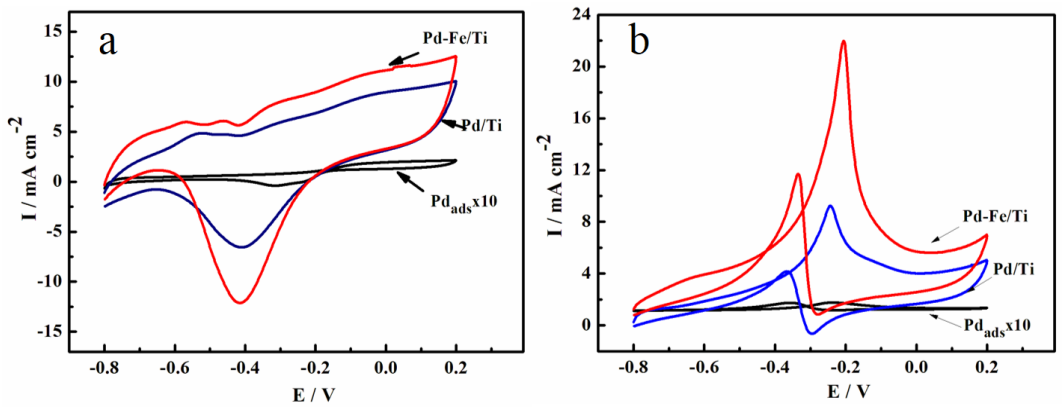

Figure 2. Cyclic voltammograms (CVs) of the different electrodes in (a) 0.5 M NaOH and (b) 0.5 M NaOH + 0.1 M glucose at a scan rate of 50 mV s^{-1}.

Fig. 2(a) presents the cyclic voltammograms (CVs) of a Pd standard electrode, the Pd/Ti electrode and Pd-Fe/Ti electrode in 0.5 M NaOH. The Pd-Fe/Ti electrode has a higher electrocatalytic activity than Pd/Ti because of its bigger electrochemically surface active areas. As shown in Fig. 2(a), it is obviously noted that the onset reduction of Pd occurs at -420 and -410 mV for the Pd-Fe/Ti and Pd/Ti electrodes, respectively. It is observed that the potential of Pd has a 10 mV negative shift and twice enhanced current densities of onset reduction. Compared with Pd/Ti electrode, the current densities of the as-synthesized Pd-Fe/Ti electrode has greatly enhanced.

For the practical applications of catalyst, Fig. 2(b) presents the CVs of three different electrodes recorded in 0.5 M NaOH + 0.1 M glucose. In the positive scan, only one oxidation peak attributed to the oxidation of glucose was observed. In the negative scan, the first peak is the reduction of Pd, followed by the oxidation of glucose on the active site which was formed in the reduction of Pd. As for the nanoporous Pd/Ti and Pd-Fe/Ti electrode, their voltammetric behaviors were superior to the Pd standard electrode, both Pd/Ti and Pd-Fe/Ti electrodes produce substantially enhanced (nearly hundreds of times) current response than Pd standard electrode, it may caused by the substrates of the nanoporous Ti plates with increased active surface area. For the comparison of Pd/Ti and Pd-Fe/Ti, the oxidation peaks current of glucose at the Pd-Fe/Ti catalyst is almost twice of Pd/Ti catalyst, which demonstrates that the Pd-Fe/Ti catalyst have a higher catalytic activity than the Pd/Ti catalyst. It is reported that the Pd-Fe catalyst presents higher catalytic activity than Pd catalyst, which is originated from the bifunctional mechanism and electronic effect [25]. To further investigate the applications in glucose sensors, Pd-Fe/Ti was chosen to construct glucose sensor.

3.3 Optimization of the operational conditions

Furthermore, amperometric responses of the Pd-Fe/Ti electrode were investigated at different potentials. For comparison, we studied the amperometric responses of the Pd-Fe/Ti electrode at the potentials of -50, -20, 0, 20 and 50 mV with successive addition of 0.1 mM glucose into 20 ml 0.5 M NaOH solution with constantly stirring (shown in Fig. 3). At all potentials, the current densities present

a typical ladder with the addition of glucose. At the potentials of -20 mV and -50 mV, the Pd- Fe/Ti electrode had stronger amperometric responses, indicating that glucose and its intermediates were able to oxidize continuously on the Pd-Fe/Ti surface more easily. In addition, the curve at the potentials of -20 mV is relatively smooth and low noise. Above all, the Pd-Fe/Ti electrode at the potentials of -20 mV showed superior performances of electro-catalytic oxidation-reduction for glucose. Therefore, we choose the potential of -20 mV as the optimal condition for glucose detection.

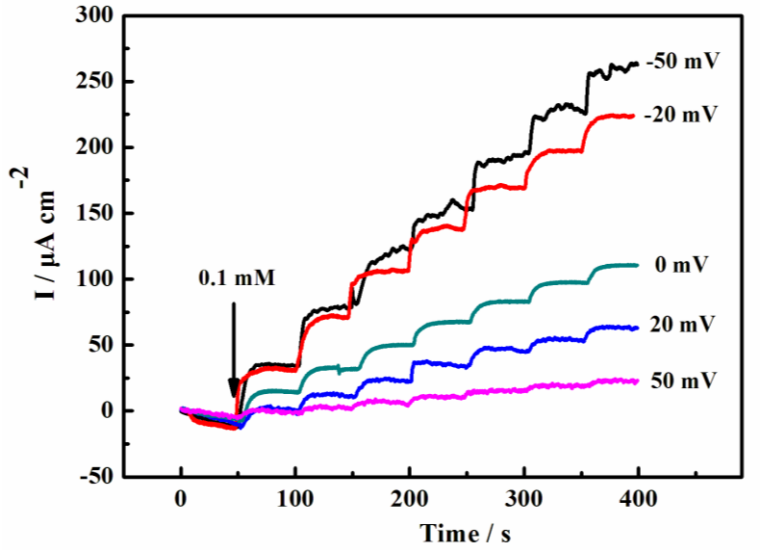

Figure 3. Amperometric responses of the Pd-Fe/Ti electrode at different detection potentials with successive addition of 0.1 mM glucose.

3.4 Anti-interferences, reproducibility and stability of Pd-Fe/Ti electrodes

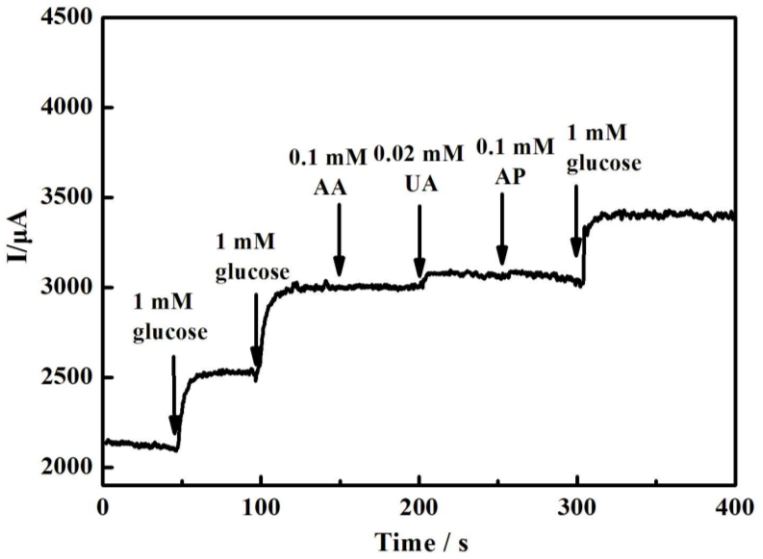

Figure 4. Amperometric responses of Pd-Fe/Ti electrode in a 0.5 M NaOH with successive addition of 0.1 mM AA, 0.02 mM UA, 0.1 mM AP, and 1 mM glucose at 50 s intervals with a potential set constant at -20 mV.

It is well known that one of the main troubles to detect glucose is the interference (for instance, AA, UA and AP). Despite the fact that glucose concentration (3 ~ 8 mM) is higher than those of ascorbic acid (AA, 0.1 mM), uric acid (UA, 0.02 mM) and 4-acetamidophenol (AP, 0.1 mM) in a normal human serum sample, these interferences can also produce oxidation currents since their faster electron transfer rates. In order to check the selectivity of this sensor, an experiment was carried out by adding 0.02 mM UA, 0.1 mM AA, 0.1 mM AP interfering agents and 1mM glucose successively into 20 ml 0.5 M NaOH solution with constantly stirring. The corresponding result is shown in Fig. 4. Interestingly, the Pd-Fe/Ti electrode emerges ignorable currents for all three interferences and still produces significant responses to increased glucose concentrations. Analysis shows that Pd-Fe/Ti electrode effectively avoided the interference from AA, UA, and AP. In short, Pd-Fe/Ti electrode presents high sensitivity and selectivity for non-enzymatic glucose sensor.

The CV peak potentials and currents were checked to study the stability of the sensor. After being kept in a refrigerator for 30 d, the peak currents retained 94.8 % of the initial value. Moreover, a good reproducibility (RSD 3.6 %) was obtained for the current response to glucose recorded on the sensors prepared independently.

3.5 Amperometric detection of glucose

Amperometry was used to study the response of Pd-Fe/Ti electrode to glucose in 0.5 M NaOH at -20 mV, with the addition of different concentration of glucose (2.0×10^{-3} to 3.0 mM). The results are clarified in Fig. 5(a). With glucose added, the current response increases linearly and the linear calibration graph is given in Fig. 5(b). The calibration data matches up linearly with the concentration range. Calculations proves that the sensor demonstrates good linearity in the range from 2.0×10^{-3} to 3.0 mM, the regression equation is I (μA) = $1.1 \times 10^{1} + 3.2 \times 10^{2}$ c (mM) and correlation coefficient is 0.9981. The sensitivity is 3.2×10^{2} μA mM^{-1} cm^{-2} with a lowest detection limit of 1.0×10^{-3} mM (S/N ratio = 3).

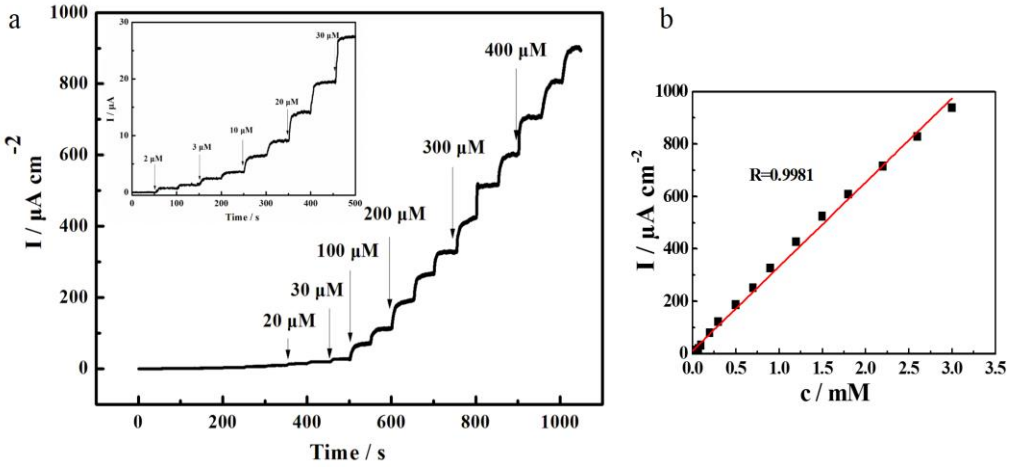

Figure 5. Amperometric response of Pd-Fe/Ti electrodes to glucose (a) and its calibration curve (b). The glucose addition each time is 2, 2, 3, 3, 10, 10, 20, 20, 30, 100, 100, 100, 200, 200, 200, 300, 300, 300, 400, 400, 400 μM.

The comparison of several electrochemical parameters between the sensor in this work and other published sensors are listed in Table 1. As can be seen, the Pd-Fe/Ti electrode showed higher sensitivity (3.2×10^2 μA mM^{-1} cm^{-2}) and a relatively low detection limit (1.0 μM) compared with others [26-29]. It is comparable to other non-enzymatic glucose sensors, no matter what based on Pd or other metals and metal oxides [30-34]. In table 1, the sensitivity of the Pd-Fe/Ti electrode is higher than most of others [35-36], this phenomenon might be attribute to high electroactive surface area of flower shaped Fe nanoparticles, the synergistic effect of Pd/Fe, and the high conductivity of Ti plate. For electrodes of the Pt-Pd nanoflakes [12] and the Ag_2O-CuO/GPE [34], although their sensitivities are higher, the detection limits are about ten times higher than the Pd-Fe/Ti electrode. Above all, the Pd-Fe/Ti electrode can be used to fabricate sensor and detect glucose of low concentration over the range from 2.0×10^{-3} to 3.0 mM.

Table 1. The comparison of some published non-enzymatic glucose sensors.

Working electrode	Sensitivity (μA mM^{-1} cm^{-2})	LOD (μM)	LDR (mM)	Reference
Pd-Fe/Ti	320	1.0	2.0×10^{-3}-3.0	This wok
Pd-modified TiO_2	290	N/A	7.0-35	[9]
Pt-Pd nanoflakes	480	21	1.0-16	[12]
Pd-Ni/SiNWs	190	2.9	0-20	[17]
Pd-Ni/Si-MCP	81	5.0	0-25	[22]
Pt-Pb/Ti	11	N/A	1.0-16	[23]
Pd/CeO_2-C	3.5	N/A	1.0-10	[26]
Pd/NiO@Nile-rGO/CPE	N/A	2.2	0.02-20	[27]
Pt-PbNPs/MWCNTs	18	1.8	0-11	[28]
Pt-Ir/Ti	94	N/A	0-20	[29]
Au-PdNWs	N/A	1.0	0.05-5 1×10^{-3}-	[30]
Ni/ITO	189	0.5	0.35	[31]
Ti/TiO_2 NTA/Ni	200	4.0	0-1.7	[32]
Pt-Cu nanochains	140	2.5	0.01-14	[33]
AgO–CuO/GPE	460	23.9	0.03-7.78	[34]
Pt/DGNs/GC	275	10	0.1-14	[35]
$Ni(OH)_2$ modified CILE	200	6.0	0.05-23	[36]

3.6 Determination of glucose in blood serum

The practical applicability of the fabricated non-enzymatic glucose sensor was investigated by the determination of glucose in human blood serum samples. 1.0 mL of blood sample was added into 19.0 mL 0.5 M NaOH under the operation potential of -20 mV. For the spike measurement, 10 μL 0.1 M glucose was added into the sample, the calculated results were shown in Table 2. Each sample was

tested five times and calculated its relative standard deviation (RSD). The data of concentration before spiking were found to be well in agreement with their real concentration and have good precision and accuracy. Good recoveries from 92 % to 108 % were obtained with the RSD less than 7 %.

Table 2. The determination results of glucose in human blood samples (n = 5).

Sample	Before spiking (mM)	Spiked (mM)	After spiking (mM)	RSD (%)	Recovery (%)
1	0.184	0.050	0.232	4.50	96
2	0.198	0.050	0.252	3.10	108
3	0.290	0.050	0.336	2.60	92

Accuracy tests were carried out by healthcare professionals in a hospital. Compared the determination results in blood samples detected from our experiments with those measured by the professionals, the calculated results were listed in Table 3. This comparison specifically indicates that our results agree well with the determination in the hospital. So the prepared sensor can be employed for determining the concentration of glucose in the practical blood samples.

Table 3. Comparison between the results obtained from the hospital and detected by present sensor for the concentration of glucose in blood samples.

Sample	Determined in hospital (mM)	Determined by our sensor (mM)	Error (mM)
1	0.172	0.184	+ 0.012
2	0.201	0.198	– 0.003
3	0.274	0.290	+ 0.016

4. CONCLUSION

In summary, three-dimensional nanoporous Pd-Fe bimetallic networks have been successfully synthesized directly on Ti plates using a one-step chemical reduction method in aqueous solutions. The Pd-Fe composites were characterized by SEM, EDS, CVs and amperometry. The Pd-Fe/Ti electrode, which is easy to fabricate, time-saving and low-cost, has significant responses to glucose. The non-enzymatic glucose sensor presents wide linearity, superior stability, high selectivity and acceptable precision. The sensitivity of this sensor is 3.2×10^{2} μA mM^{-1} cm^{-2} range from 2.0×10^{-3} to 3.0 mM, the detection limit was found to be 1.0×10^{-3} mM (S/N = 3). Furthermore, it can be applied to the determination of glucose in human blood samples. This study demonstrates that the Pd-Fe/Ti electrode possess potential application for the preparation of non-enzyme glucose sensors for practical analysis.

ACKNOWLEDGEMENTS
This work was supported by the National Natural Science Foundation of China (Grant Nos.21375116), a project funded by the Priority Academic Program Development of Jiangsu Higher Education Institutions.

References

1. A. L. Galant, R. C. Kaufman, J. D. Wilson, *Food. Chem.,* 188 (2015) 149.
2. S. Mittelmaier, M. Funfrocken, D. Fenn, T. Ficjhert, M. Pischetsriederet, *J. Chromatogr. B,* 878 (2010) 877.
3. R. Z. Hu, Y. H. Weng, L. M. Lai, J. C. Chen, Q. Lin, *Chromatographia*, 57 (2003) 471.
4. C. L. Yang, X. H. Zhang, G. Lan, L. Y. Chen, M. W. Chen, Y. Q. Zeng, J. Q. Jiang, *Chin. Chem. Lett.*, 25 (2014) 496.
5. S. J. Li, N. Xia, B. Q. Yuan, W. M. Du, Z. F. Sun, B. B. Zhou, *Electrochim. Acta,* 159 (2015) 234.
6. E. Bakker, *Anal. Chem.,* 76 (2004) 3285.
7. W. Q. Wu, Y. B. Li, J. Y. Jin, H. M. Wu, S. F. Wang, Q. H. Xia, *Sensor. Actuat. B-Chem.,* 232 (2016) 633.
8. D. Rathod, C. Dickinson, D. Egan, *Sensor. Actuat. B-Chem.,* 143 (2010) 547.
9. Q. F. Yi, F. J. Niu, W. Q. Yu, *Thin Solid Films,* 519 (2011) 3155.
10. K. Nikolaev, S. Ermakov, Y. Ermolenko, E. Averyaskina, A. Offenhäusser, *Bioelectrochemistry,* 105 (2015) 34.
11. J. Wang, *Chem. Rev.,* 108 (2008) 814.
12. X. Niu, M. Lan, C. Chen, H. L. Zhao, *Talanta,* 99 (2012) 1062.
13. X. L. Chena, H. B. Pana, H. F. Liua, M. Dua, *Electrochim. Acta,* 56 (2010) 636.
14. Y. P. Sun, H. Buck, T. E. Mallouk, *Anal. Chem.*, 73 (2001) 1599.
15. B. Fang, A. X. Gu, G. F. Wang, W. Wang, Y. H. Feng, C. H. Zhang, X. J. Zhang, *ACS Appl. Mater. Inter.,* 1 (2009) 2829.
16. H. Xu, K. Malladi, C. L. Wang, L. Kulinsky, M. J. Song, M. Madou, *Biosens. Bioelectron.,* 23 (2008) 1637.
17. S. C. Hui, J. Zhang, X. J. Chen, H. H. Xu, D. F. Ma, Y. L. Liu, B. R. Tao, *Sensor. Actuat. B-Chem.,* 155 (2011) 592.
18. Y. Q. Zhang, Y. Z. Wang, J. B. Jia, J. G. Wang, *Sensor. Actuat. B-Chem.***, 171 (2012) 580.**
19. K. Dhara, R. Thiagarajan, B. G. Nair, G. S. B. Thekkedath, *Microchim. Acta,* 182 (2015) 2183.
20. M. R. Guascito, D. Chirizzi, C. Malitesta, M. Siciliano, T. Siciliano, A. Tepore, *Electrochem. Commun.,* 22 (2012) 45.
21. J. H. Yuan, K. Wang, X. H. Xia, *Adv. Funct. Mater.,* 15 (2005) 803-809.
22. F. J. Miao, B. R. Tao, L. Sun, T. Liu, J. C. You, L. W. Wang, P. K. Chu, *Sensor. Actuat. B-Chem.,* 141 (2009) 338.
23. J. P. Wang, D. F. Thomas, A. C. Chen, *Anal. Chem.,* 80 (2008) 997.
24. W. Z. Wang, B. Poudel, Z. F. Ren, *J. Phys. Chem. B*, 110 (2006) 25702.
25. Y. L. Han, C. J. Liu, J. Hoeita, W. L. Yan, *Appl. Catal. B Environ.,* 188 (2016) 77.
26. S. Q. Song, K. Wang, L. L. Yan, A. Brouzgou, Y. L. Zhang, Y. Wang, P. Tsiakaras, *Appl. Catal. B Environ.,* 176 (2015) 233.
27. A. A. Ensafi, Z. Ahmadi, J. A. Mehdi, B. Rezaei, *Electrochim. Acta,* 173 (2015) 619.
28. H. F. Cui, J. S. Ye, W. D. Zhang, C. M. Li, J. H. T. Luong, F. S. Sheu, *Anal. Chim. Acta,* 594 (2007) 175.
29. P. Holt-Hindle, S. Nigro, M. Asmussen, A. C. Chen, *Electrochem. Commun.,* 10 (2008) 1438.
30. M. Zhang, F. L. Cheng, Z. Q. Cai, H. J. Yao, *Int. J. Electrochem. Sci.,* 5 (2010) 1026.
31. H. F. Tian, M. Z. Jia, M. X. Zhang, J. B. Hua, *Electrochim. Acta,* 96 (2013) 285

32. C. X. Wang, L. W. Yin, L. Y. Zhang, R. Gao, *J. Phys. Chem. C,* 114(2010) 4408.
33. X. Cao, N. Wang, S. Jia, Y. Shao, *Anal. Chem.,* 85 (2013) 5040.
34. J. Orozco, C. Fernández-Sánchez, E. Mendoza, M. Baeza, F. Céspedes, C. Jiménez-Jorquera, *Anal. Chim. Acta,* 607 (2008) 176.
35. H. M. Jia, G. Chang, M. Lei, H. P. He, X. Liu, H. H. Shu, T. T. Xia, J. Su, Y. B. He, *Appl. Surf. Sci.,* 384 (2016) 58.
36. A. Safavi, N. Maleki, E. Farjami, *Biosens. Bioelectron.,* 24 (2009) 1655.

© 2017 The Authors. Published by ESG (www.electrochemsci.org). This article is an open access article distributed under the terms and conditions of the Creative Commons Attribution license (http://creativecommons.org/licenses/by/4.0/).